

The X-ray afterglow of GRB000926 observed by BeppoSAX and Chandra: a mildly collimated fireball in a dense medium ?

L. Piro¹, G. Garmire², M. R. Garcia³, L. A. Antonelli⁴, E. Costa¹, M. Feroci¹, D. A. Frail⁵,
F. Harrison⁶, K. Hurley⁷, P. Mészáros², E. Waxman⁸

Received _____; accepted _____

Accepted for publication in ApJ

¹Istituto Astrofisica Spaziale, C.N.R., Via Fosso del Cavaliere, 00133 Roma, Italy

²Department of Astronomy and Astrophysics, 525 Davey Lab, Penn State University, University Park, PA 16802, USA

³Harvard-Smithsonian Center for Astrophysics, 60 Garden St. Cambridge, MA 02138, USA

⁴Osservatorio Astronomico Roma, Via Frascati 33, 00040 Monte Porzio Catone, Roma, Italy

⁵NRAO, 1003 Lopezville Rd., Socorro, NM 87801, USA

⁶California Institute of Technology, Pasadena, CA, 91125, USA

⁷UC Space Science Laboratory, Berkeley, CA 94720-7450, USA

⁸Weizmann Institute, Rehovot 76100, Israel

ABSTRACT

We present X-ray observations of the afterglow of GRB000926 performed around and after the break observed in the optical light curve two days after the burst. The steep X-ray light curve observed around the break confirms the presence of this feature in X-rays. However, the spectral and temporal properties are not consistent with a standard jet scenario based on synchrotron emission, requiring a more complicated model. We find that X-ray and optical data are compatible with a moderately collimated fireball (with opening angle $\theta \approx 25^\circ$) expanding in a dense medium ($n \approx 4 \times 10^4 \text{ cm}^{-3}$). This produces two breaks in the light curve. The first, at $t \approx 2$ days, is due to jet behavior. The second, around 5 days, is attributed to the transition of the fireball to a non-relativistic expansion. This transition predicts a *flattening* of the light curve, that explains the late X-ray measurement in excess above the extrapolation of the simple jet scenario, and is also consistent with optical data.

Subject headings: gamma rays: bursts

1. Introduction

Afterglows of Gamma Ray Bursts (GRB) are typically characterized by a power law behavior in time and in frequency, i.e. the observed flux $F \approx (t - t_0)^{-\delta} \nu^{-\alpha}$. This property is nicely accounted for by the fireball model, in which the afterglow is produced by the interaction of a relativistic expanding shell with an external medium (e.g. Wijers, Rees & Mészáros 1997). The spectral and temporal slopes depend on the geometry (e.g. spherical vs jet (Sari, Piran & Halpern 1999)) and on the density distribution of the external medium (e.g. constant density – hereafter ISM – vs. wind (Chevalier & Li 1999)). A change of the slope (i.e. a break) of the light curve is produced either when a spectral break (like that associated to ν_c , the cooling frequency of electrons) transits the observed frequency window or when “bulk” variations,- i.e. global changes of the kinematics or hydrodynamics of the fireball,- take place. The latter is the case of jet expansion or the transition from relativistic to non-relativistic expansion (hereafter named NRE). In contrast to the effect of spectral breaks, jet expansion and NRE produce achromatic breaks in the light curves. In a jet this happens when the beaming angle of the fireball ($\approx \Gamma^{-1}$, where Γ is the Lorentz factor), becomes similar to the opening angle of the jet, θ (Sari, Piran & Halpern 1999, Roads 1999), at the time t_θ :

$$t_\theta \approx (1 + z) \left(\frac{E_{i,53}}{n} \right)^{1/3} \left(\frac{\theta}{0.1} \right)^{8/3} \text{days}, \quad (1)$$

where $n = n_6 \text{ } 10^6 \text{cm}^{-3}$ is the density and $E_i = E_{i,53} \text{ } 10^{53} \text{ erg s}^{-1}$ is the energy the fireball would have if it were spherically symmetric; i.e., in the case of a jet of solid angle $\Delta\Omega$, its energy would be $E = \frac{\Delta\Omega}{4\pi} E_i$.

The transition to NRE instead occurs when the blast wave has swept up a rest-mass energy equal to its initial energy, at a time (e.g. Wijers, Rees & Mészáros 1997, Livio &

Waxman (2000), hereafter LW):

$$t_{NRE} \approx 3 \frac{1+z}{2} \left(\frac{E_{53}}{n_6} \right)^{1/3} \text{days} \quad (2)$$

Both jet and NRE can therefore yield achromatic breaks a few days after the burst. The NRE requires an external medium of a much higher density than that of a jet. This is indeed what one would expect if GRB originate in dense star forming regions, a scenario for which supporting evidence is accumulating (e.g. Piro *et al.* 2000a, Kulkarni *et al.* 2000).

So far, evidence of achromatic breaks has been claimed in some optical afterglows (e.g. Harrison *et al.* 1999, Kulkarni *et al.* 1999), but an *unambiguous* detection of this feature in the X-ray range is still missing (e.g. Kuulkers *et al.* 2000, Pian *et al.* 2001). Most of the authors attribute this feature to jet behavior, although this model may have some problem in accounting for the sharpness of the transition (Rhoads & Fruchter 2001). In fact, there is no - a priori - reason to exclude a NRE and there is at least one case (GRB990123) in which it has been attributed to either cases (Kulkarni *et al.* 1999, Dai & Lu 1999). In GRB000926 a break in the optical light curve at $t \approx 2$ days has been reported by several groups (Fynbo *et al.* 2000b, Veillet 2000, Halpern *et al.* 2000, Rol *et al.* 2000, Price *et al.* (2000, hereafter P0). The observed variation of the temporal slope of ≈ 2 is much larger than the value of 0.25 expected by a spectral break (Sari, Piran & Halpern 1999). Indeed, a jet scenario has been proposed to explain this behavior (P0).

In this paper we report on BeppoSAX and Chandra observations of the afterglow of this burst (Sect. 2 & 3). Those observation occurred around and after the break observed in the optical. We compare X-ray with optical data (Sect.4) and show that they are explained by jet behavior *and* a NRE into a high density medium.

2. Observations, data analysis and the X-ray spectrum

The gamma-ray burst GRB000926 was detected by the Interplanetary Network (IPN) on $t_0 = \text{Sep.26.99 U.T.}$ (Hurley *et al.* 2000). It was a moderately bright GRB, with a revised 25-100 keV fluence of $6.2 \times 10^{-6} \text{erg cm}^{-2}$, and a duration of about 25 s (Hurley *et al.* 2000). Optical observations (Dall *et al.* 2000, Gorosabel *et al.* 2000) showed an optical counterpart, at a very bright level ($R = 19.3$) one day after the GRB. This is the second brightest afterglow ever observed in the optical band. This finding triggered two rapid target of opportunity observations in X-rays, one with BeppoSAX and the other with Chandra. A second Chandra observation was scheduled around $t = t_0 + 12$ days, to study the late time evolution of the afterglow.

The BeppoSAX (Piro, Scarsi & Butler 1995, Boella *et al.* 1997) observation started on Sep. 29.03 ($t - t_0 = 2$ days) and lasted for 12 hrs. Effective exposure times were 20 ksec for the MECS(1.6-10 keV) and 5 ksec for the LECS(0.1-10 keV). The analysis of the MECS image showed a previously unknown fading source in a position consistent, within the error of $50''$, with the optical transient, and therefore identified as the X-ray afterglow of GRB000926 (Piro *et al.* 2000b, Piro *et al.* 2000c). The source was only marginally detected in the LECS. The average count rate of the source in the MECS(1.6-10 keV) is $(3.2 \pm 0.6) \times 10^{-3} \text{cts/s}$. The spectrum is well fitted by a power law with energy index $\alpha = (0.9 \pm 0.7)^9$ and absorption by our Galaxy ($N_H = 2.7 \times 10^{20} \text{cm}^{-2}$) and $F(1.6-10 \text{ keV}) = F(0.2-5 \text{ keV}) = (2.6 \pm 0.6) \times 10^{-13} \text{erg cm}^{-2} \text{s}^{-1}$. We have checked different background subtraction methods, finding that the corresponding systematic effect amount to less than about 15%. This has been included in the flux error quoted above.

⁹ Hereafter errors and upper limits on fit parameters, including temporal slopes, correspond to 90% confidence level for one parameter of interest

A Chandra X-ray Observatory (Weisskopf *et al.* 1996) TOO observation (hereafter C1) with the ACIS-S began on Sep. 29.674 ($t - t_0 = 2.7$ days) and ended on Sep. 29.851, with an exposure time of 10ks. The X-ray afterglow was observed at a position RA(2000)=17h 04m 09.6s; Decl. (2000)= +51 47' 8.6" with an uncertainty of 2", consistent with the optical position. The source count rate in the 0.3-5 keV range is $(2.9 \pm 0.2) \times 10^{-2}$ cts s^{-1} , corresponding to a flux $F(0.2-5 \text{ keV}) = (1.2 \pm 1.0) \times 10^{-13} \text{ erg cm}^{-2} \text{ s}^{-1}$ for the best fit power law spectrum. This has $\alpha = (0.8 \pm 0.2)$, i.e. consistent with the BeppoSAX slope, and absorption $N_H = (5 \pm 3) \times 10^{20} \text{ cm}^{-2}$, consistent with that of our Galaxy. Since the BeppoSAX and Chandra spectral shapes are consistent, we have fitted them simultaneously linking the spectral parameters (but for the normalizations). We obtain a good fit ($\chi^2 = 25.6, \nu = 26$) with $\alpha = 0.85 \pm 0.15$, a ratio of the BeppoSAX over Chandra normalization of 2.3 ± 0.6 and some marginal evidence of intrinsic absorption (in addition to the one in our Galaxy) in the rest frame of the GRB ($z=2.06$ Fynbo *et al.* 2000a, Castro *et al.* 2000)), corresponding to a column density $N_{HGRB} = (0.4^{+0.35}_{-0.25}) \times 10^{22} \text{ cm}^{-2}$. The residuals around 2 keV, i.e. the iron line region in the rest frame of the GRB (Fig.1), are marginal, with an upper limit on an iron line of $I < 2 \times 10^{-5} \text{ cm}^{-2} \text{ s}^{-1}$, corresponding to an equivalent width $EW < 1 \text{ keV}$. For comparison, the iron line detected by Chandra in GRB991216 has $EW = 0.5 \text{ keV}$ (Piro *et al.* 2000a).

The last Chandra observation (hereafter C2) took place on Oct.10.176 and ended on Oct. 10.58. The afterglow count rate had faded to $2.0 \pm 0.75 \times 10^{-3} \text{ cs}^{-1}$ (0.3–5.0 keV), allowing ~ 60 counts to be collected in the 33 ksec exposure. With so few counts it is difficult to place good constraints on N_H and α simultaneously, so we fix $N_{HGRB} = 0$ (or $0.4 \times 10^{22} \text{ cm}^{-2}$) and find $\alpha = 0.85 \pm 0.15$ (or 1.2 ± 0.3). The flux in the 0.2-5 keV range derived by the best fit power law is equal in both cases to $(8.3 \pm 1.1) \times 10^{-15} \text{ erg cm}^{-2} \text{ s}^{-1}$. An overall fit on the three data sets (see Fig. 1) gives $\chi^2/\nu = 30.8/24$, with spectral parameters consistent with those derived previously (see the inset in Fig.1) and a ratio of the normalizations C2/C1 of

$(7.7 \pm 1.1) \times 10^{-2}$.

We find marginal evidence of a steeper spectrum in C2. The ratio of count rates in the 0.2-1.5 keV range over 1.5-8 keV is in fact 2.1 ± 0.6 and 3.9 ± 0.2 in C1 and C2 respectively. If we leave the slope of C2 unlinked in the combined fit of all data sets, we get $\alpha_{C2} = 1.23 \pm 0.3$. While this result is of marginal statistical significance, it is interesting to note that the difference in slope between C2 and C1+BeppoSAX is $\Delta\alpha = 0.4 \pm 0.3$, i.e. consistent with the steepening of 1/2 expected when ν_c passes into the energy window.

An intrinsic column density $N_{HGRB} \approx 0.4 \times 10^{22} \text{cm}^{-2}$ is marginally detected at a confidence level of $\approx 98\%$ (see the inset in Fig.1). We remark that, since most of the local gas is ionized by GRB photons (Boettcher *et al.* 1999), the real column density can be much higher. Assuming that the relation between the optical extinction A_V and N_H is similar to that in our own galaxy (e.g. Predehl & Schmitt 1995), gives $A_v \approx 2$. This value is $\approx 2 - 20$ greater than that derived by optical measurements (P0), implying a dust-to-gas ratio much lower than that of our Galaxy. This effect has been observed in other GRB (Galama & Wijers 2000) and it may be the result of destruction of dust by the GRB radiation (Waxman & Draine 2000).

3. A very steep X-ray decay

In the BeppoSAX data the source exhibits a substantial decay, decreasing by a factor of (1.7 ± 0.5) in 6 hours. This corresponds to a power law decay $F \propto (t - t_0)^{-\delta_X}$ with slope $\delta_X \approx 4$. This behaviour is consistent with the first Chandra observation, that took place near the end of the BeppoSAX observation, and whose flux was a factor 2.3 ± 0.6 times lower than the average BeppoSAX flux. Combining these two data sets (Fig.2) we derive a slope $\delta_X = 3.7_{-1.6}^{+1.3}$, in agreement with the optical slope measured after the break. The late

Chandra point appears to deviate from this law, the slope connecting C1 with C2 being $\delta_x = 1.70 \pm 0.16$. However, when the large error of the earlier slope is considered, the two measurements are nearly compatible (Fig. 2). A combined fit to all the X-ray data points gives then $\delta_X = 1.89_{-0.16}^{+0.19}$ with $F(2-10 \text{ keV}) = 1.19 \times 10^{-12} \text{ erg cm}^{-2} \text{ s}^{-1}$ at $t = 1$ day.

The X-ray decay of GRB000926 is much steeper than that typically observed in X-ray afterglows, where $\delta_X \approx 1.4$ (Piro 2000). We remark, however, that previous observations covered the evolution of the afterglow primarily at $t - t_0 < 2$ days. The data presented here are instead sampling the X-ray behaviour at later times. It is in this domain that we expect deviations due to either a jet or NRE.

4. Jet vs NRE of a spherical fireball in a dense medium

The optical data (Fig.2) are nicely fitted by the standard jet model with synchrotron emission (P0) but, when X-ray data are considered, we find inconsistencies with this scenario. The relationship linking the temporal and spectral slopes are (Sari, Piran & Halpern 1999) $\delta = 2\alpha + 1$ ($\nu < \nu_c$) and $\delta = 2\alpha$ ($\nu > \nu_c$). We find then that the X-ray temporal and spectral slopes $\delta_X = 1.9$ and $\alpha_x = 0.85$ are consistent only with the case of a cooling frequency below the X-ray range. The slope p of the electron distribution $N_e \propto \gamma^{-p}$ would then be $p = \delta = 2\alpha = 1.7 \pm 0.3$, i.e. marginally compatible with the minimum slope needed to avoid an infinite energy content in electrons. A more relevant problem of this model is that the predicted temporal slope is significantly lower than the one measured in optical (P0; see also Fig. 1), $\delta_O = 2.3 \pm 0.08$. Furthermore, the electron slope derived from the optical data under the same scenario ($p = 2.39 \pm 0.15$) is not consistent with the X-ray derivation. Finally we note that the - admittedly marginal - evidence of a spectral steepening in C2, argues against a jet behavior, during which ν_c remains constant.

We now examine the alternative explanation of a transition to NRE of a spherical fireball . The relationships linking δ and α are given in Livio & Waxman (2000). We find that the X-ray data are consistent with a NRE either in a uniform density medium (which gives $\delta = 2.17 \pm 0.45$) or in a wind ($\delta = 2.3 \pm 0.35$). The cooling frequency is now *above* the X-ray range, and therefore $p = 2.7 \pm 0.3$. In this case the optical and X-ray spectral data points should lie on a single power law. We have evaluated the slope $\alpha_{OX} = -\frac{\log(F_X/F_O)}{\log(\nu_X/\nu_O)}$ of the power law connecting the flux at 1 keV observed by Chandra (F_X) with the R band flux extrapolated at the time of the Chandra observation (F_O , Fig.2) and corrected for the extinction (P0). We find $\alpha_{OX} = 0.9 - 1.1$, in agreement with the slope measured in X-rays. Before the break the evolution is indistinguishable from that of a spherical relativistic fireball, which follows a decay with $\delta = 1.3 \pm 0.2$ (ISM) or $\delta = 1.8 \pm 0.2$ (wind). The latter case is not compatible with the optical slope measured before the break (P0), and we conclude that both optical and X-ray data are consistent with a spherical expansion in a uniform medium, with the temporal break produced by a transition to NRE. From eq.(2) we derive $n_6 \approx 10$. We have estimated, following Freedman and Waxman (2000), a fireball energy comparable to the observed γ -ray isotropic energy, which is $E_{i,\gamma} = 8 \times 10^{52}$ erg ($z = 2.03$ (Castro *et al.* 2000), $H_0 = 75$ km/s/Mpc, $q_0 = 1/2$). The absorbing column density is $N_H \approx nr_{NRE} \approx 10^{23}$ cm⁻², where the radius $r_{NRE} \approx 10^{16}$ cm (LW). This is in apparent disagreement with the upper limits derived by the X-ray spectrum. This disagreement is rectified by recalling that the medium is heavily ionized by the GRB photons, and therefore its effective absorption is negligible (Boettcher *et al.* 1999).

5. A collimated fireball in a dense medium

There remains, however, a discrepancy between optical and X-ray data, that is not accounted for by previous models. The X-ray decay *after* the break ($\delta_X = 1.70 \pm 0.16$) is

significantly flatter than the optical one ($\delta_O = 2.30 \pm 0.08$, P0). In fact, the extrapolation of the X-ray flux with the optical slope at the time of the second Chandra observation underestimates the observed flux by a factor of 2 ± 0.5 (Fig.2). This indicates the presence of a *flattening* taking place in between the two sets of observations, as predicted in the case of a jet expansion followed by a transition to NRE(LW). In this case, the lateral expansion of the jet begins when it is relativistic, and during the lateral expansion stage there is rapid decline of the flux due to the rapid decrease of the fireball energy per unit solid angle (as this angle increases). This is producing the first break in the light curve. The time at which the jet completes its side-ways expansion, is roughly the same time at which the flow becomes sub-relativistic. At this stage, lateral expansion is no longer important, and the rapid flux decline due to lateral expansion ceases, leading to a flattening of the light curve. This effect appears more evident in X-rays, which are not contaminated at later times by the presence of a fairly bright host galaxy (P0).

We show now that both optical and X-ray data are in agreement with this scenario. The light curve of the afterglow is composed by three subsequent power laws with decay slopes δ_1 , δ_2 , and δ_3 , that we have modeled with the empirical formula :

$$F(t) = F(t_{b1}) \frac{[(\frac{t}{t_{b1}})^{\delta_1 s} + (\frac{t}{t_{b1}})^{\delta_2 s}]^{-1/s}}{[1 + (\frac{t}{t_{b2}})^{\delta_2 s}]^{-1/s} [1 + (\frac{t}{t_{b2}})^{\delta_3 s}]^{1/s}} \quad (3)$$

The parameter s describes the sharpness of the breaks. The temporal slopes are related to the power law index of electrons by relationships that depend on the location of ν_c and on the density distribution of the external medium (LW). We can exclude most of the cases as follows. $\alpha_{OX} \approx \alpha_x$ implies that ν_c is either below the optical or above the X-ray range. In the first case, we would have $p = 2\alpha_X = 1.7$ that, besides being less than 2, would give temporal slopes flatter than observed. In fact: $\delta_1 = \frac{(3p-2)}{4} = 0.8$, $\delta_2 = p = 1.7$ and $\delta_3 = 1 + \frac{7}{6}(p-2) = 0.65$ (wind) or $\delta_3 = 1 + \frac{3}{2}(p-2) = 0.55$ (ISM). During the jet phase

$\nu_c = const$ while, in the NRE phase, ν_c increases (decreases) with time for a wind (ISM). In the case of a wind ν_c could move above the optical range, but still giving a flat slope $\delta_3 = \frac{3}{2} + \frac{7}{6}(p - 2) = 1.15$.

Let us now examine the case of ν_c lying above the X-ray range. This implies $p = 2\alpha_X + 1 = 2.7$. The case of a wind is excluded because $\delta_1 = 1.8$, i.e. greater than observed. For a ISM we have $\delta_1 = \frac{3}{4}(p - 1) = 1.3$, $\delta_2 = p = 2.7$ and $\delta_3 = \frac{9}{10} + \frac{3}{2}(p - 2) = 1.95$, which appear to be consistent with the data. We have assessed this case more quantitatively by fitting eq.(3), with the slopes expressed as a function of p , to the optical data (with the contribution of the host galaxy subtracted) . We obtain $p = 2.57 \pm 0.3$, in nice agreement with the value derived from the X-ray spectra, $t_{b1} = 1.76^{+0.7}_{-0.4}$ days, $t_{b2} = 5.5 \pm 2$ days, and $s = 1.7 \pm 0.3$. Moreover, this same law (i.e. rescaling the normalization but with the same parameters determined by the optical light curve) fits fairly well all the X-ray data points, and in particular reproduce C2 (Fig. 3). We also note that this law predicts a temporal slope of about 2.6 around 2 days, nearer to the steep decay observed in the BeppoSAX an C1 observations.

The simultaneous determination of $t_\theta = t_{b1}$ and $t_{NRE} = t_{b2}$ allows an unambiguous determination (i.e. not depending on estimates of E_i and n) of the jet angle (LW). In fact $t_{NRE} = (1 + z)^{3/4} (\frac{E_{i,53}}{n_6})^{1/4} t_\theta^{1/4}$ which, when combined with eq.(1), gives $\theta = 0.7 (\frac{t_\theta}{t_{NRE}})^{1/2} = 0.4$. The total γ -ray energy is then, for a two-sided jet, $E_\gamma = 0.16 E_{\gamma,i} = 1.2 \times 10^{52} \text{erg s}^{-1}$. Finally, the density $n_6 = (1 + z)^3 E_{i,53} \frac{t_\theta}{t_{NRE}^4} \approx 0.04$. Note that the jet angle is rather insensitive to the errors in the determination of break times. Conversely, the density should be considered as an order of magnitude estimate, due to the strong dependence on t_{NRE} and to model details (LW). We have finally checked whether the value of density is compatible with the broad band spectrum of the GRB, following the prescriptions of Wijers & Galama (1999). Since the parameters one derives

are dependent on the model adopted, we have restricted the analysis to the data before the break, when the fireball evolution is indistinguishable from the spherical case. From the radio data (Frail, private communication; Harrison *et al.* (2001)) and the extrapolation of the optical-to-X-ray spectrum at lower frequencies, we derive that the synchrotron self-absorption frequency ν_a and frequency of the maximum flux ν_m should be in the range between $10^{10} - 10^{12}$ Hz, and that the flux at ν_m should be \approx a few mJy. Furthermore, as we have shown before, $\nu_c \gtrsim 10^{18}$ Hz. The large range spanned by these quantities gives a density spread over orders of magnitude that, however, comfortably include the density estimate derived before.

6. Conclusions

In this paper we have shown that X-ray observations of the afterglow of GRB000926 around and after the break observed in the optical confirm the presence of this feature in X-rays as well. However, they are not consistent with the standard jet scenario based on synchrotron emission, requiring a more complicated model. We find that both the spectral and temporal properties of X-ray and optical data are compatible with a moderately collimated fireball ($\theta \approx 25^\circ$) expanding in a dense medium ($n \approx 4 \times 10^4 \text{ cm}^{-3}$). This produces two breaks in the light curve. The first is due, as usual, to a jet behavior. The second, around 5 days, is attributed to a transition to NRE due to the high density of the external medium, and is followed by a *flattening* of the curve, that accounts for the late X-ray measurement, and is also preferred by optical data. Optical measurements at later times should help to characterize this behavior but, to do so, it will be necessary to actually single out the afterglow from the host in the image. Current estimates of the contribution of the host galaxy from the flattening exhibited by the light curve will, in fact, cancel out any intrinsic flattening due to the afterglow. Finally, we note that we cannot exclude other

possibilities like, for example, an event of gravitational lensing (Mao & Loeb 2001) that amplified the flux around 12 days, or a contribution of an Inverse Compton component to the late X-ray emission (Harrison *et al.* 2001). An analysis of different options goes, however, beyond the scope of this paper.

Our result supports the association of GRB with star forming regions. In fact, the density is consistent with that of very dense molecular clouds ($n \approx 10^4 \text{ cm}^{-3}$). On the other hand it is not as high as that required to produce the iron lines observed in some X-ray afterglows (e.g. Antonelli *et al.* 2001; Piro *et al.* 2000a and references therein), which is possibly connected with much denser ($n \approx 10^{10} \text{ cm}^{-3}$) progenitor ejecta. In these cases the environment must be composed by at least two regions, since the fireball requires a medium with a density $n \lesssim 10^7 \text{ cm}^{-3}$ to produce an afterglow lasting at least a few days. The properties of this medium, in particular the density, are not the same in all GRB. While in this GRB we find $n \approx 4 \times 10^4 \text{ cm}^{-3}$, in several other GRB the density should be much lower, as indicated, for example, by the absence of breaks in the optical light curves (Kulkarni *et al.* 2000) or by the evidence of relativistic expansion several weeks after the GRB (Waxman, Kulkarni & Frail 1998). Another element of diversity in GRB appears to be the magnetic field strength. In this burst the magnetic field density is estimated to be less than $\approx 10^{-6}$ times the equipartition value, comparable to that of GRB971214 (Wijers & Galama 1999) and GRB990123 (Galama *et al.* 1999), but four orders of magnitude weaker than in GRB970508 (Wijers & Galama 1999). As suggested by Galama *et al.* (1999), such differences in field strength may reflect differences in energy flow from the central engine.

We thank the BeppoSAX & Chandra teams for the support, in particular H. Tananbaum for the organization of the Chandra TOO. BeppoSAX is a program of the Italian space agency (ASI) with participation of the Dutch space agency (NIVR). KH is grateful for Ulysses support under JPL contract NAG 5-9503, and for NEAR support under

NASA grant NAG5-95903. GG & PM acknowledge support under NASA grant G00-1010X. MRG acknowledges support under NASA contract NAG8-39073 to the Chandra X-Ray Center.

REFERENCES

- Antonelli L.A., *et al.* 2001, ApJ, in press (astro-ph/0010221)
- Boella G., Butler R.C., Perola G.C., Piro L. & Bleeker J.A.M. 1997, A&AS122, 299
- Boettcher M., Dermer C.D.D., Crider A. W. & Liang E.D. 1999, A&A343, 111
- Castro S. *et al.* 2000, GCN n. 851
- Chevalier R. & Li Z.-Y. 1999, ApJ, 520, L29
- Dai, Z. G. & Lu T. 1999, ApJ519, L155
- Dall T. *et al.* 2000, GCN n. 804
- Freedman D. L. & Waxman E. 2001 ApJ, 547, 922
- Fynbo J.P.U. *et al.* 2000a, GCN n. 807
- Fynbo J.P.U. *et al.* 2000b, GCN n. 820 & 840
- Galama T. *et al.* , 1999, Nature , , 398, 394
- Galama, T. J. & Wijers R. A.M.J. 2000, ApJ, in press (astro-ph/0009367)
- Gorosabel J. *et al.* 2000, GCN n. 803
- Halpern J.P., *et al.* 2000, GCN n. 824 & 829
- Harrison F. *et al.* 1999, ApJ523, L121
- Harrison F. *et al.* 2001, ApJ, subm. (astro-ph/0103377)
- Hurley K. *et al.* GCN n.801 & 802 (2000).
- Kulkarni S. *et al.* 1999, Nature , 398, 389

- Kulkarni S. *et al.* 2000, proc. of V Hunstsville Symposium on GRB, 18-22 Oct. 1999, R.M. Kippen, R.S. Mallozzi & G.J Fishman ed.s., AIP Vol. 526, p.277
- Kuulkers *et al.* 2000, ApJ, 538, 638
- Livio M. & Waxman E. 2000, ApJ, 538, 187 (LW)
- Mao S. & Loeb A. 2001, ApJ, 547, L97
- Pian E. *et al.* 2001, A&A, submitted (astro-ph/0012107)
- Piro L., Scarsi L. & Butler R.C. 1995, proc. of SPIE conf. on X-Ray and EUV/FUV spectroscopy and Polarimetry, Vol. 2517, p.169
- Piro L., *et al.* . 2000, Science 290, 955
- Piro L. & BeppoSAX team 2000a, GCN n. 832
- Piro L., Antonelli L., & BeppoSAX team 2000b, GCN n.832, 833
- Piro L. 2000, Proc.s. of "X-Ray Astronomy '99: Stellar Endpoints, AGN and the Diffuse X-ray Background", September 6-10, 1999, CNR Bologna (astro-ph/0001436)
- Predehl, P. & Schmitt J. H.M. M. 1995, A&A293, 889
- Price P.A. *et al.* 2000, ApJ, in press (astro-ph/0012303) (P0)
- Roads, J.E. 1999 ApJ, 525, 737
- Rhoads J.E. & Fruchter A.S. 2001, ApJ, 546, 117
- Rol E. *et al.* 2000, GCN n.850
- Sari R., Piran T. & Halpern J.P. 1999, ApJ, 519, L17
- Veillet C. 2000, GCN n.823 & 831

Waxman, E. & Draine , B.T. 2000, ApJ523, 796

Waxman E., Kulkarni S. R. & Frail D. A. 1998, ApJ, 497, 288

Weisskopf, M. C. , O’Dell, S. & van Speybroeck, L. P. *Proc of Multilayer and Grazing Incidence X-Ray/EUV Optics III* (eds R. B. Hoover and A. B. Walker), 2 (SPIE, 2805, 1996).

Wijers, R.A.M.J., Rees, M.J. & Mészáros P. 1997, MNRAS288, L51

Wijers, R.A.M.J., & Galama T.J 1999, ApJ523, 177

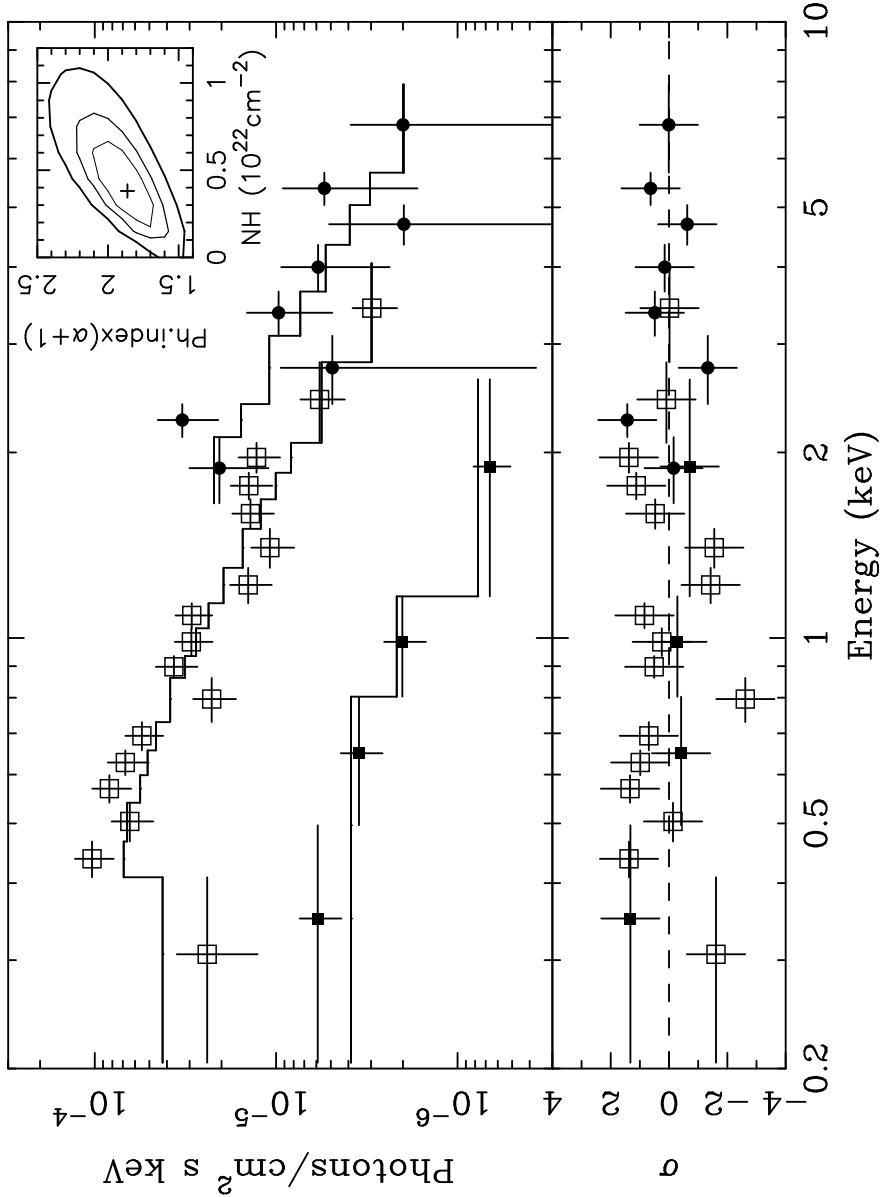


Fig. 1.— The X-ray spectrum of the afterglow of GRB000926 as observed by the ACIS-S of Chandra (first observation: open squares; second observation: filled squares) and the MECS of BeppoSAX (filled circles; the LECS is not shown for clarity). The continuous lines represent the best fit power law convoluted through instrument responses. Deviations from the best fit in σ are plotted in the lower panel. In the inset we show the the contour plot of the photon index ($\alpha + 1$) vs N_H with the 99% (thick line) , 90% (medium-thick line) and 68% (thin line) confidence regions

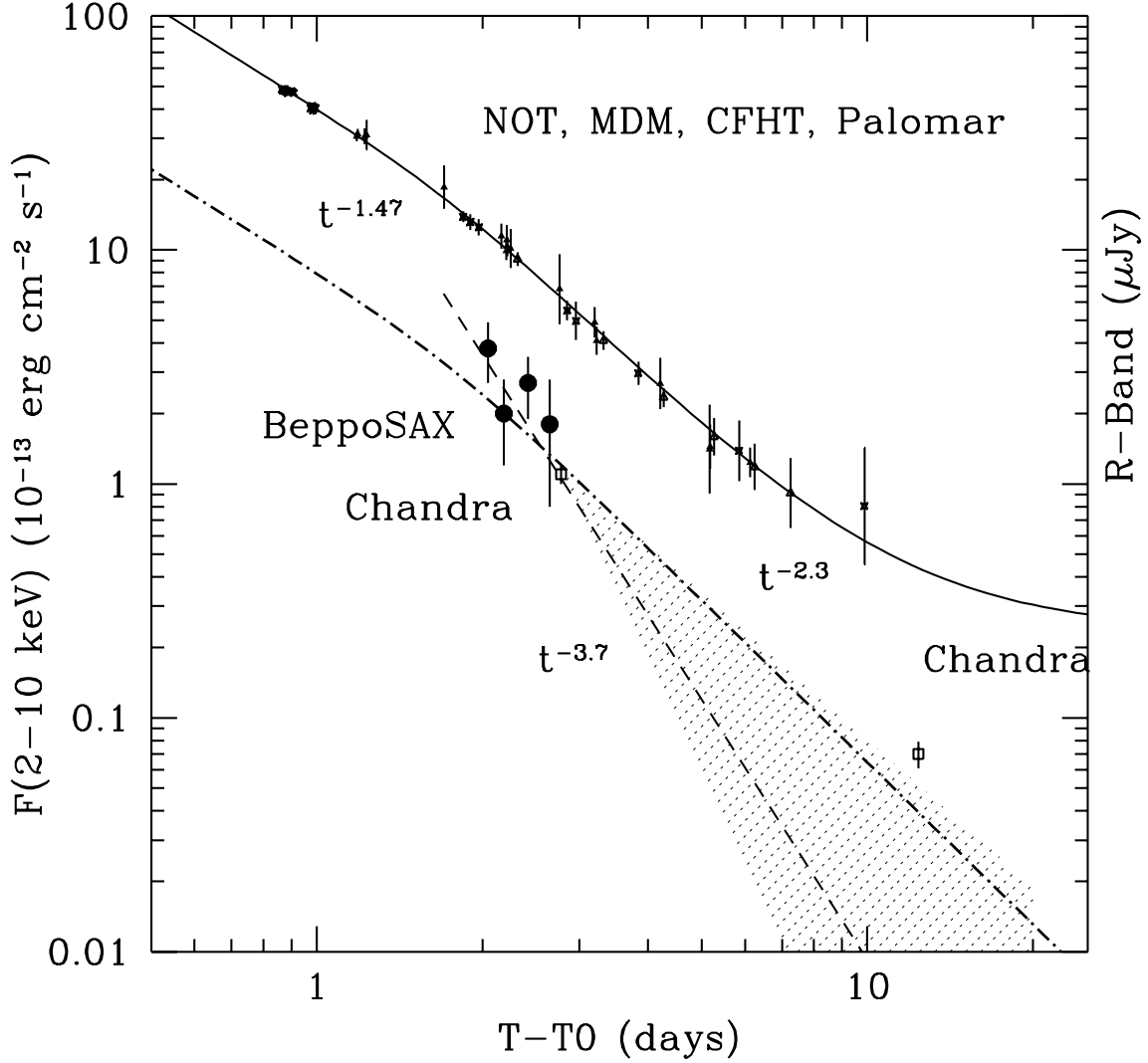


Fig. 2.— The X-ray and optical (R band) light curves of the afterglow of GRB000926. Optical data are from Dall *et al.* (2000), Fynbo *et al.* (2000a, 2000b), Halpern *et al.* (2000), Price *et al.* (2000), Veillet *et al.* (2000). The X-ray light curves have been derived by converting the flux at 1 keV, which is not significantly dependent on the spectral shape, to the F(2-10) keV flux, by adopting the best fit power law with $\alpha = 0.85$ for all the spectra. The dashed line is the best fit to the data of the BeppoSAX and first Chandra observations. The allowed region (at 90% confidence level) obtained by extrapolating the previous fit is identified with the shaded area. The continuous line is the best fit to the optical data including the effect of the host galaxy (P0). The dash-dot line is the template of the optical afterglow (obtained from the best fit to the data subtracting the galaxy) normalized to the

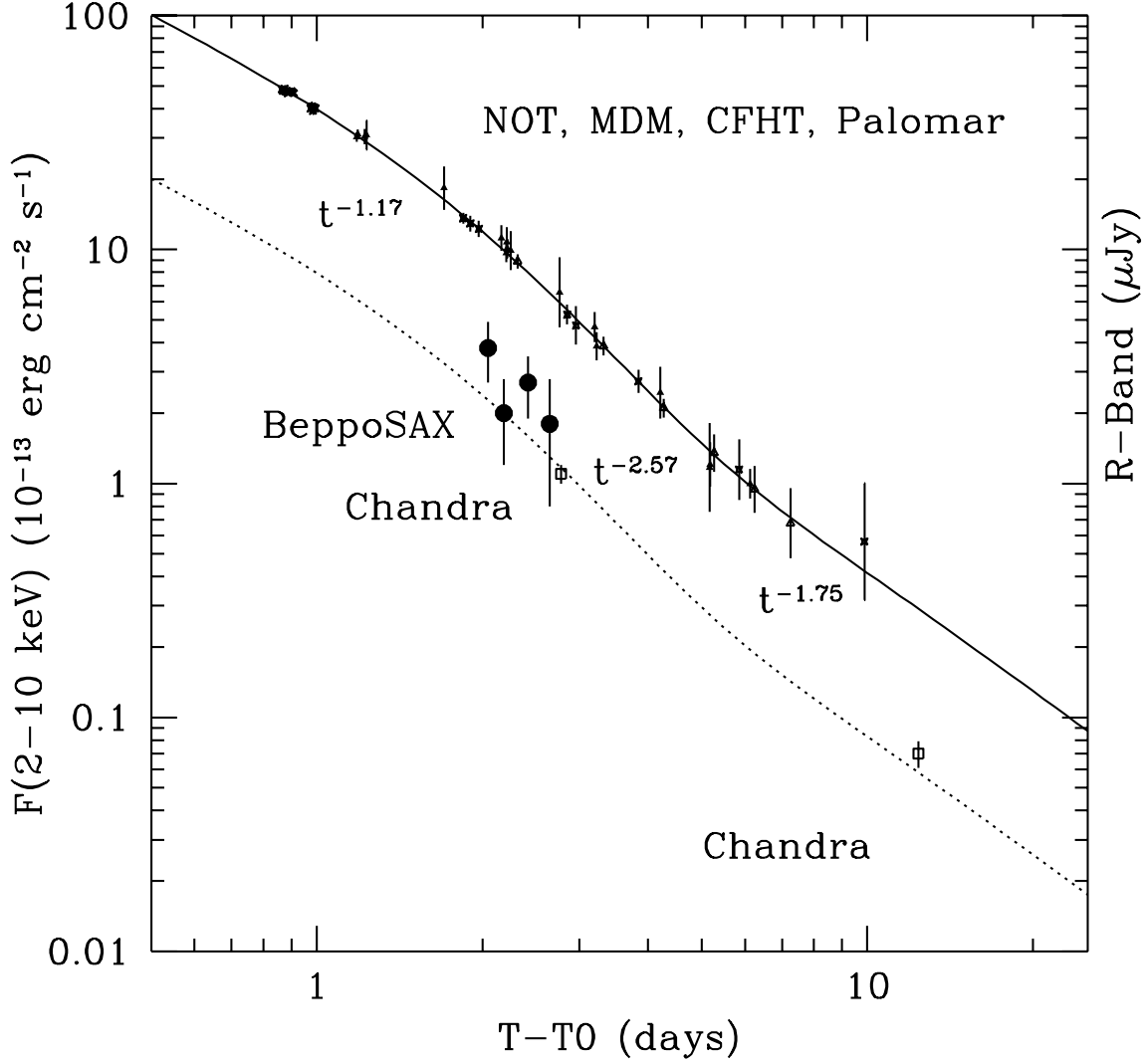


Fig. 3.— Same as in Fig.2 but with the contribution of the galaxy subtracted from optical data. The continuous and dotted light curves represent the expected behaviour in the case of a moderately collimated jet with a transition to non-relativistic expansion at $t=5.5$ days. Note the flattening of light curves both in the optical and X-rays after this second break.